RESEARCH PAPER

FLASH FLOOD HAZARD MAPPING USING LANDSAT-8 IMAGERY, AHP, AND GIS IN THE NGAN SAU AND NGAN PHO RIVER BASINS, NORTH-CENTRAL VIETNAM

Tien-thanh Nguyen[1*], Anh-huy Hoang[2], Thi-thu-huong Pham[1], Thi-thu-trang Tran[1]
[1]Faculty of Surveying, Mapping, and Geographic Information, Hanoi University of Natural Resources and Environment, 41A, Phu Dien Road, North-Tu Liem District, Hanoi, 100000, Vietnam
[2]Faculty of Environment, Hanoi University of Natural Resources and Environment, 41A, Phu Dien Road, North-Tu Liem District, Hanoi, 100000, Vietnam
*Corresponding author: ntthanh@hunre.edu.vn

ABSTRACT. Flash floods have been blamed for significant losses and destruction all around the world are widely, including Vietnam, a developing nation that has been particularly hard hit by climate change. Therefore, flash flood hazards are essential for reducing flood risks. The topographic wetness index (TWI), altitude, slope, aspect, rainfall, land cover, normalized difference vegetation index (NDVI), distances to rivers and roads, and flow length were used in this study to create a spatial database of ten exploratory factors influencing the occurrence of flash floods in the Ngan Sau and Ngan Pho river basins (North-Central Vietnam). Subsequently, the analytic hierarchy process (AHP) was applied to calculate the weights of these influencing factors. The flood threat was then mapped using GIS techniques. The validation of the flash flood hazards involved 151 flood inventory sites in total. The findings demonstrate that (i) distance from rivers (0.14) and TWI (0.14) factors have the greatest influence on flash flooding, whereas distance from roads (0.06) and NDVI (0.06) factors were found to have the least influence; (ii) a good conformity of 84.8 percent between flood inventory sites and moderate to very high levels of flash flood hazard areas was also discovered; (iii) high and very high flood hazard levels covering areas of 275 and 621.1 km^2 were mainly detected along and close to the main rivers and streams, respectively. These results demonstrated the effectiveness of GIS techniques, AHP, and Landsat-8 remote sensing data for flash flood hazard mapping.

KEYWORDS: flash floods, hazard mapping, GIS techniques, AHP, remote sensing, Ngan Sau and Ngan Pho river basin (Vietnam)

Conflict of interests: The authors reported no potential conflict of interest.

INTRODUCTION

Flood represents the excess flow that inundates the conveying or holding medium when its capacity has been exceeded (Getahun and Gebre 2015). This is the most frequently occurring natural disaster in the world (Jonkman 2005), which has caused millions of fatalities in the twentieth century, tens of billions of dollars of direct economic loss each year, and serious disruption to global trade (Merz et al. 2021). Recently, Kvočka et al. (2016) generally characterized four types of flood events as extreme flood events, including dam-break floods, storm surges, flash floods, and extreme/large river floods. Among these types of extreme flood events, flash floods are one of the most significant natural hazards that cause serious

risk to life and destruction of buildings and infrastructure (Gaume et al. 2009) and pose the greatest flood risk to the general population (Kvočka et al. 2016). According to a research by Chatzichristaki et al. (2015), areas with increased housing development such as tourist destinations and places near city centres, where the stream bed is severely affected by human pressure, are more likely to experience flood fatalities. Due to the increasingly devastating effects of floods, the recent year's scientific community has drawn attention for the identification of flood-exposed areas and particularly critical infrastructure and assets in flood hazard zone (Qiang 2019; Stefanidis et al. 2022). Therefore, flood risk assessment, including three approaches of hazard, exposure, and vulnerability assessment as proposed by Field et al. (2012), plays a vital role in flood prevention and

flood risk management. Among these approaches, flood hazard assessment usually receives the most attention as flood hazard maps are used for estimating the danger to people due to flooding (Koks et al. 2015).

Over the years, a lot of work has gone into developing methods for effective flood hazard mapping. Teng et al. (2017) summarizes flood hazard mapping can be carried out based on three major approaches, namely the physically-based, empirical, and physical modelling methods. A review of the most recent studies by Mudashiru et al. (2021) has indicated an application rate of 43.8% for physically based, 10% for physical, and 46.2% for the empirical modelling methods in flood hazard mapping. This shows that the use of empirical modelling methods has received a lot of attention in flood hazard mapping. The empirical models are data-driven models, popularly referred to as black-box models that rely on observation data and characteristics and mechanisms of the hydrological cycle Mudashiru et al. (2021). Chen et al. (2019) divided empirical models for flood modeling and mapping into qualitative and quantitative methods. The quantitative-based empirical models depend upon data analysis targeted at evaluating the relationship between flood occurrence and flood-causing/contributing factors, while the qualitative approach relies upon experts' opinions of the same (Mudashiru et al. 2021). With the help of a Geographic Information System (GIS), one of the main advantages of empirical models is their operability with various statistical and data-driven approaches through the use of different types of data such as Digital Elevation Model (DEM), terrain, hydrological and geomorphology data, and remotely sensed images. These data-driven approaches for flood hazard mapping are categorized into multi-criteria decision-making modelling methods (Arabameri et al. 2019; Mudashiru et al. 2022), statistical modelling methods (Arabameri et al. 2019; Malik et al. 2021), artificial intelligence (Chang et al. 2020; Chapi et al. 2017), machine learning models (Hosseini et al. 2020; Rahman, Chen, et al. 2021), and the state-of-the-art deep learning models (Costache et al. 2022; Satarzadeh et al. 2022). Among these approaches, a combination of GIS with a multi-criteria decision-making modelling method-based analytic hierarchy process (GIS-AHP) has proved its effectiveness in many recent studies on flood hazard

mapping (Aydin and Sevgi Birincioğlu 2022; Daneshparvar et al. 2022; Pathan et al. 2022). In addition, a recent study of Şahin (2021) has revealed that the most important benefit of AHP over other multi-criteria decision-making modelling methods is that it not only allows pairwise comparisons, which increase the accuracy of judgments compared to evaluating all the alternatives simultaneously, but also permits consistency checking. Despite numerous studies, there hasn't been much research done on mapping flash flood hazards using a combination of remote sensing, GIS, and AHP techniques. To fill this literature gap, this paper aims to investigate the use of Landsat-8 imagery, AHP, and GIS in identifying the flash flood influencing factors and map flood hazards.

Disastrous flooding is projected to increase in many regions, particularly in Africa and Asia (Merz et al. 2021). As a country situated in Asia, Vietnam frequently experiences extreme weather-related natural disasters (Noy and Vu 2010), of which flooding in North-Central Vietnam is the most serious (Bich et al. 2011). The Ngan Sau and Ngan Pho river basins, which are in North-Central Vietnam, are frequently the area most affected by floods (Kha et al. 2018; Long and Dung 2009; Nguyen and Ha 2017). Therefore, the objective of this study is to investigate the integration of Landsat-8 imagery, AHP, and GIS in mapping flash flood hazards in the study area.

STUDY AREA AND DATA USED

Study area

Geographically, the study area of the Ngan Sau and Ngan Pho river basins is located between 17°50´00´´N to 18°37´58´´N latitudes and 105°07´00´´E to 106°56´00´´E longitudes, covering an area of approximately 4,274 square kilometers (Fig. 1). Politically, the Ngan Sau and Ngan Pho river basins consist of Huong Son, Duc Tho, Vu Quang, and Huong Khe districts, which are located in Ha Tinh administrative province (Fig. 1-b), North-Central Vietnam (Fig. 1-a). The Ngan Pho river basin covers an area of 1,060 km² with a river and stream density of 0.91 km/km² and a total volume of water of 1.40 km³ corresponding to an average flow of 45.6 m³/s (Tran et al. 2020). Whereas the Ngan Sau river system is the second largest tributary of the Ca river,
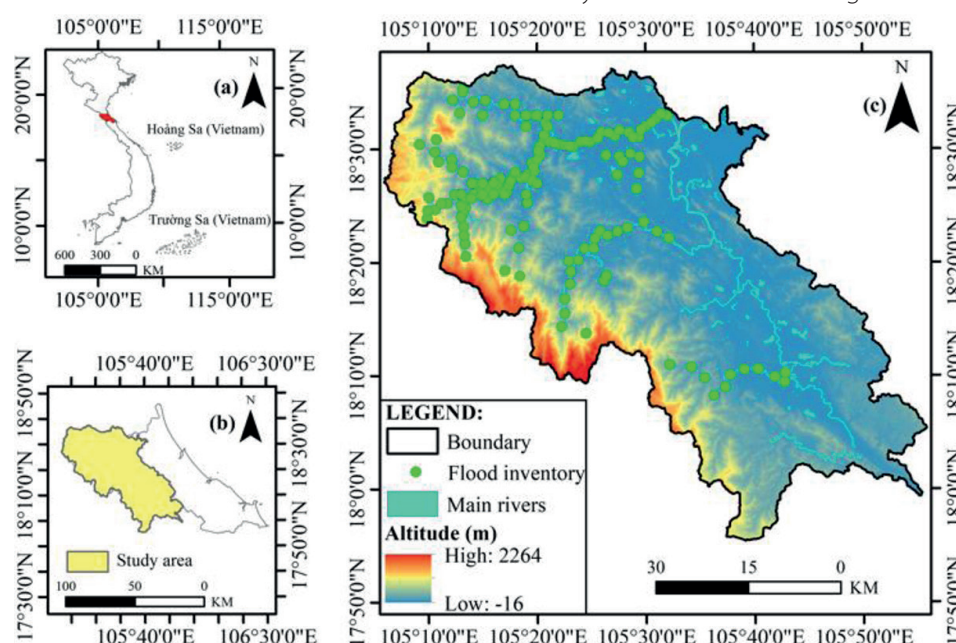

Fig. 1. Location of the study area: (a) location of Ha Tinh province (North-Central Vietnam), (b) location of Ngan Sau-Ngan Pho River basin, (c) altitude of Ngan Sau-Ngan Pho River basin overlaid by flood inventory sites and main rivers and streams

extending 135 km (Hoang et al. 2020). The study area's relief is low in the north and northeast, increasing towards the west and southwest at as high as 2264 m (Fig. 1-c).

In the Ngan Sau and Ngan Pho river basins, which were among the floodplains in central Vietnam that were most severely affected (Kha et al. 2018; Long and Dung 2009; Nguyen and Ha 2017; Nguyen 2017), flash floods have been blamed for several fatalities and significant environmental and societal harm. Typically, ten deaths, 16,200 households flooded, 177 houses washed away, and 5,026 hectares of winter-spring rice crops were damaged by a flash flood in the upstream area of the Ngan Pho River basin in 1989 (Hoang et al. 2020). Also in this upstream area, heavy rain caused another flash flood in 2002. A total of 77 deaths, hundreds of injuries, and 70,694 houses flooded were also reported in a recent study of Hoang et al. (2020). In addition, loss of life, social-economic and environmental damages caused by other flash floods were also confirmed in recent years (Hoang and Tran 2018; Nguyen and Ha 2017).

Data used

In this study, Landsat-8 Collection 2 Level 2 Science Product (L2SP) (paths of 126 and 127, rows of 47 and 48) recently distributed by the United States Geological Survey (USGS) website (www.usgs.gov) was acquired on April 8, 2022. Landsat-8 L2SP with a spatial resolution of 30 meters provides surface reflectance data that is already atmospherically corrected (Marzouki and Dridri 2022). These Landsat-8 L2SP images were used to extract land cover types and NDVI. Thirty-meter resolution DEM datasets downloaded from the USGS were used to calculate topographic and

hydrologic parameters (slope, aspect, TWI, flow length, flow direction, flow accumulation, and stream networks). Rainfall data was obtained from the CRU (Climate Research Unit) website (https://crudata.uea.ac.uk). The road network layer and 151 flood inventory sites were obtained from the project (grant number: TNMT.2016.05.12), which was financially supported by the Ministry-level Scientific and Technological Key Programs of the Ministry of Natural Resources and Environment of Vietnam. The road network layer was used to calculate the distance to roads, whereas flood inventory sites were used for the validation of the flash flood hazards.

METHODOLOGY

Data from Fig. 2 demonstrates the workflow of this study. The input data (flood inventory and ten exploratory factors) was first collected and prepared in ArcGIS. Among these factors, land cover types and NDVI were extracted from Landsat-8 OLI imagery in ENVI. Subsequently, the weights of the flood conditioning factors were calculated using the AHP technique. Then, GIS techniques were applied to categorize flash flood hazards into five levels: very low, low, moderate, high, and very high. Finally, the validation of flash flood hazards was carried out based on the test data values of 151 flood inventory sites.

Selection of influencing factors

In this study, based on the causes of flash floods reported previously and the important characteristics of the Ngan Sau and Ngan Pho river basins such as natural conditions, topography and hydro-meteorology, a total
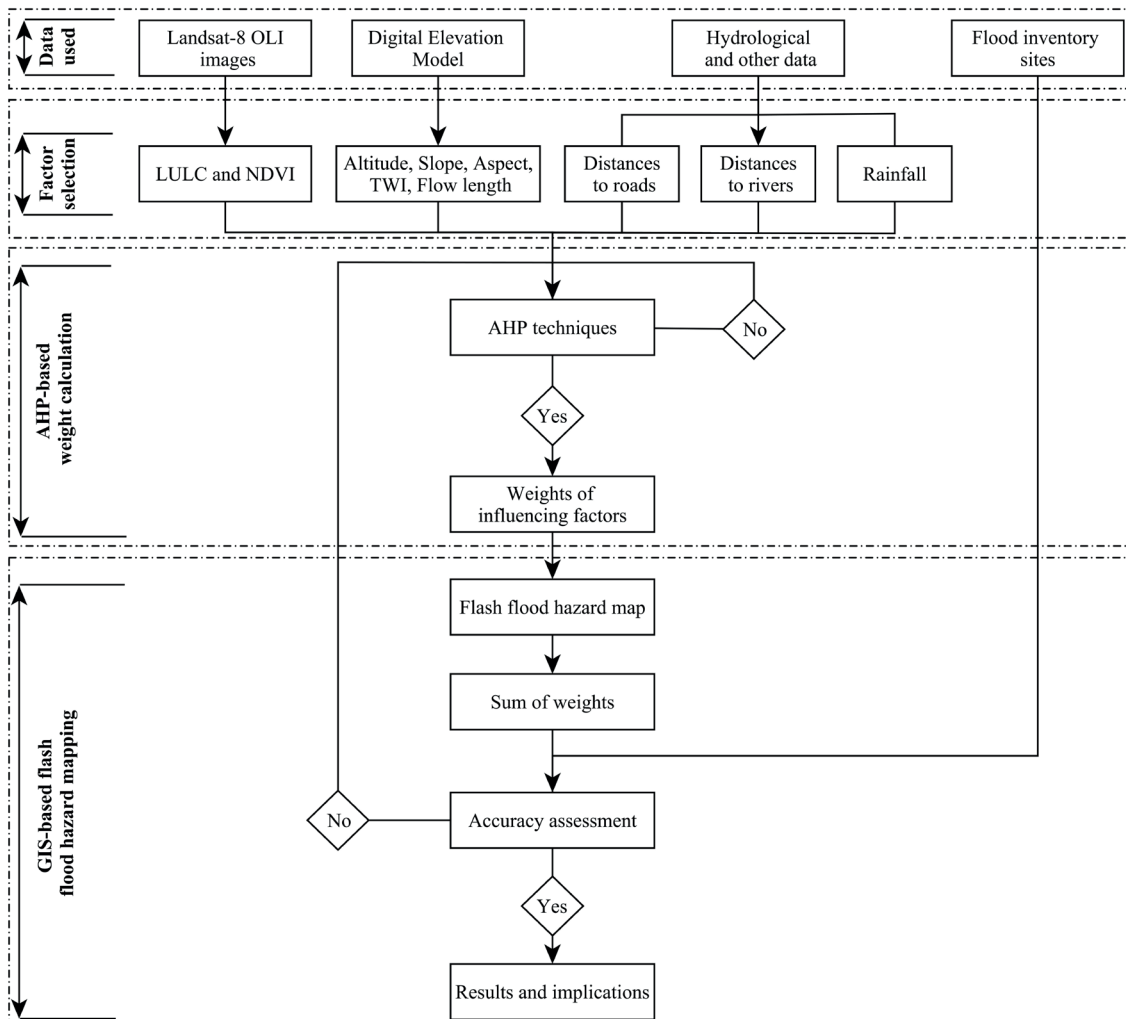

Fig. 2. Workflow of this study

59

of ten major flash flood hazard-influencing factors were chosen to investigate the effectiveness of the proposed method. These factors include altitude, slope, aspect, TWI, land cover, NDVI, distances to rivers and roads, rainfall, and flow length.

The topographic factors, including altitude, slope, aspect, and TWI, play significant roles in flood hazard mapping. The altitude of the Ngan Sau and Ngan Pho river basins varies from 16 meters to 2264 meters (Fig. 3-b) and was derived from DEM (acquired from the USGS). Flood hazard and altitude are inversely proportional, which indicate that relatively more elevated areas are relatively less susceptible to floods (Rahman and Ningsheng et al. 2021). Aspect and slope were derived from DEM data. Aspect reflects the direction of the terrain and then the direction of floodwater flow (Bui et al. 2020), whereas, the slope is a significant factor in flood mapping. The TWI factor measures the direction and accumulation of water flow due to the gravity of the place (Tehrany et al. 2015) and is calculated by equation (1):

$$TWI = \ln\left(\frac{A_s}{\tan\beta}\right) \tag{1}$$

where: A_s is the upslope area per unit of contour length (m^2/m) and β measures the topographic gradient or local slope gradient in degrees (Park and Kim 2019).

Rainfall is the main factor contributing to flooding in the Ngan Sau and Ngan Pho river basins. Most of the rainfall occurs in the monsoon season from August to October. Rainfall data was first obtained from the CRU (Climate Research Unit) website. The inverse distance weighted interpolation method in ArcGIS software was then applied to obtain the thirty-meter resolution rainfall data of the Ngan Sau and Ngan Pho river basins.

Land cover-related factors such as land cover types and NDVI are crucial factors in flood hazard mapping because areas with relatively less vegetation are often more prone to flooding (Rahman and Ningsheng et al. 2021). In this study, both land cover types and NDVI were generated from Landsat-8 OLI images in ENVI software. Based on the supervised method of maximum likelihood supervised classification, the land cover in the study area was classified into five categories: water bodies, built-up, bare land, agricultural land, and forest, respectively. Whereas the NDVI is calculated using bands 4 (red band) and 5 (near infrared band) in a Landsat-8 OLI image. The NDVI can be expressed in equation (2) (Alvarez-Mendoza et al. 2019):

$$NDVI = \frac{Band5 - Band4}{Band5 + Band4} \tag{2}$$

Distances to rivers and roads also play significant roles in the mapping of flash flood hazards. These distances can be calculated using the Euclidean distance. Areas close to main channels are more likely to be flooded (Chowdhuri et al. 2020), whereas impermeable surfaces (roadways, pavements, and parking spaces) increase the rainfall-runoff process (Mukherjee and Singh 2020).

Flow length is considered to be an important factor in flood susceptibility assessment. Flow length would be used to extract the surface runoff (Abou El-Magd et al. 2010). High surface runoff increases flood risk (Prokešová et al. 2022). Based on DEM data, it was possible to calculate the flow length within each cell, which is either equal to the grid cell length (L) in the case of orthogonal or L√2 in the case of diagonal (Abou El-Magd et al. 2010).

Analytic hierarchy process (AHP)

The AHP, first introduced by Saaty (1988), is a geospatial technique for determining the weights of the influencing factors (Rehman et al. 2022). Numerous studies have successfully applied the AHP for hazard mapping (Gigović et al. 2017; Koem and Tantanee 2021; Neji et al. 2021). In particular, AHP assembled with GIS (GIS-AHP) not only effectively provides a wide range of geographically spatial data manipulation costs and time, but also offers procedures and techniques to evaluate, to analyze, to design, and to prioritize value judgments (Rehman et al. 2022). Therefore, GIS-AHP was used in this study for the calculation of the weights of the ten flash flood hazard influencing factors.

AHP evaluates two influencing factors simultaneously, and gives preference to one factor over another based on experienced judgments. These judgments are measured using a preference scale of 1 to 9, in which a lower number (1) indicates a lesser preference and a higher number (9) shows more importance of that particular factor over another (Rehman et al. 2022). The accuracy and consistency of the obtained weights can be assessed based on the Consistency Ratio (CR). The CR is calculated by equation (3):

$$CR = \frac{CI}{RI} \tag{3}$$

where: CR is the consistency ratio of a particular AHP matrix, the Consistency Index (CI) can be calculated from equation (4), and RI is the random index.

$$RI = \frac{\lambda_{max} - n}{n - 1} \tag{4}$$

where: λ_{max} is the consistency vector, and "n" represents the number of influencing factors (n = 10 in this study). The CR should be within the limits of 10% (CR < 0.01), otherwise the assigned score values should be reconsidered (Arabameri et al. 2019; Lootsma 1999).

GIS-based flash flood hazard mapping

After weights of influencing factors were obtained, the weighted sum tool in ArcGIS software was used to multiply the designated field values for each input raster by the obtained weight. The overall weight for the final map of flash flood hazards was then synthesized using equation (5):

$$FFHI = \sum_{i=1}^{n} H_i \times W_i \tag{5}$$

where: FFHI is the flash flood hazard index, n represents the number of influencing factors, H_i is the rescaled values of influencing factor i, and W_i is the weight of the influencing factor i.

FFHI ranges from 0 to 5. Based on values of FFHI, levels of flash flood hazards in the Ngan Sau and Ngan Pho river basins were classified into five classes: very low (less than 1), low (between 1 and 2), moderate (between 2 and 3), high (between 3 and 4), and very high (more than 4).

Accuracy assessment

The areas of flash flood hazards were finally validated based on 151 flood inventory sites collected from the field survey. The accuracy assessment was performed using ArcGIS software. The layer of flood inventory sites is laid over that of flash flood hazard

areas which were obtained from the above-discussed method. The degree of spatial correlation or conformity between the areas of medium-to-high hazard levels and flood inventory is the basis for evaluating the accuracy of the proposed method. In this case, the accuracy of the proposed method increases with the increasing spatial correlation or conformance.

RESULTS AND DISCUSSIONS

Analysis of influencing factors

After datasets were collected, based on the maximum and minimum values of ten factors affecting flash flood hazards, the values of these factors were divided into 5 equal intervals or classes. The degree of these influencing factors affecting flooding was then ranked using a 1 to 5 scale or class. Class 1 represents the factor having the least influence, whereas class 5 represents the factor having the most influence. Data from Table 1 illustrates the degree of influence on flash floods of ten influencing factors in the Ngan Sau and Ngan Pho river basins.

The TWI ranged from 2 to 24.9 (Fig. 3-a). The TWI ranged between 11 and 15, and between 15 and 24.9 had the highest weight, demonstrating high and very high flood susceptibility at this range of TWI (Fig. 4-a). Whereas very low and low flood susceptibility were found with the TWI of between 2 and 5.8, and between 5.8 and 7.9. Low altitude areas, such as flat areas, foothills, and valley floors, are more susceptible to flooding (Rahman and Chen et al. 2021). The altitude ranging from -16 to 2264 meters (Fig. 3-b), was accordingly classified into five classes (Table 1). The altitude ranging between -16 and 145, 145 and 379, 379 and 717, 717 and 1155, and 1155 and 2264 meters, indicates very low, low, moderate, high, and very high influence on floods, respectively (Fig. 4-b). A low slope gradient, usually flat areas, is more susceptible to flooding (Rahman and Chen et al. 2021). The slope gradient ranged from 0 to 86.8 degrees (Fig. 3-c), and five classes of 0-6.8, 6.8-14.6, 14.6-22.1, 22.1-31, and 31-86.8 were classified (Fig. 4-c). In the case of aspect, based on the flow of main streams and rivers, the eastern-facing slopes (east, northeast, and southeast) showed a positive correlation with the flooding, hence these aspects were classified as class numbers 5 and 4 (Fig. 4-h). In contrast, the western-facing slopes (northwest, southwest, and west) indicated a weaker relationship with the flooding, with class numbers of 2 and 1, respectively. Whereas the flat areas showed the strongest relationship with flooding, therefore the flat area was classified as class 5.

Areas close to rivers and roads are more likely to be flooded (Chowdhuri et al. 2020), hence distances close to rivers and roads were assigned high-class numbers. In the case of distance to rivers, class numbers 5 and 4 were found within distances of below 778 and 778-1622 meters, followed by 1622-2587, 2587-4070, and above 4070 meters as class numbers 3, 2, and 1, respectively (Fig. 4-f). As for the factor of distance to roads, class numbers 5 and 4 were found within distances of below 3402 and 3402-7793 meters, followed by the 7793-12842, 12842-18769, and above 18769 meters as class numbers 3, 2, and 1, respectively (Fig/ 4-g). In this study, three types of land cover (Fig. 3-d), namely, water bodies, agricultural and bare lands, were found to be more susceptible to flood occurrence, whereas, other land cover types were found to have a weaker relationship with flooding. Therefore, the highest-class numbers 5 and 4 were assigned to water bodies and agricultural land, followed by bare soil, built-up, and forest as class numbers 3, 2, and 1, respectively (Fig. 4-d). The derived NDVI ranges between -0.11 and 0.65 (Fig. 3-e). The low values of NDVI indicate the less dense vegetated areas, which are more susceptible to flooding. Accordingly, the high-class numbers 5 and 4 were assigned to NDVI in the range between -0.1 and 0.14, 0.14 and 0.25, followed by the NDVI in the range of 0.25-0.3, 0.3-0.4, and 0.4-0.65 as class numbers 3, 2 and 1, respectively (Fig. 4-e).

Rainfall is an important factor that is positively correlated with flooding in the Ngan Sau and Ngan Pho river basins. In this study, the high rainfall areas were classified as high-class numbers. In this case, high-class numbers 5 and 4 were assigned to rainfall between 1736 and 1772, and between 1717 and 1736 mm, followed by the rainfall between 1697-1717, 1675-1697, and 1646-1675 mm, assigned as class numbers of 3, 2 and 1, respectively. The flow length ranged between 0 and 120594 (Fig. 3-i). High-class numbers 5 and 4 were assigned to flow length between 93272-120594 and 70189-93272, followed by the rainfall between 50875-70189, 27793-50875, and below 27793 were assigned as class numbers 3, 2, and 1, respectively.

Analysis of weights of influencing factors

In this study, the experts give their opinions and compare the pairwise influencing factors either jointly or individually. It is, accordingly, based on the experienced judgments of the

Table 1. Flash flood hazard influencing factors

No	Influencing factors	Classes (degree of influence)				
		1 (very low)	2 (low)	3 (moderate)	4 (high)	5 (very high)
1	Altitude (m)	-16-145	145-379	379-717	717-1155	1155-2264
2	Slope (degree)	0-6.8	6.8-14.6	14.6-22.1	22.1-31	31-86.8
3	Aspect	West	Northwest, Southwest	North, South	Northeast, Southeast	Flat, East
4	TWI	2-5.8	5.8-7.9	7.9-11	11-15	15-24.9
5	Flow length	0-27793	27793-50875	50875-70189	70189-93272	93272-120594
6	Distance to streams (m)	4070-9321	2587-4070	1622-2587	778-1622	0-778
7	Distance to roads (m)	18769-27989	12842-18769	7793-12842	3402-7793	0-3402
8	Rainfall (mm)	1646-1675	1675-1697	1697-1717	1717-1736	1736-1772
9	LULC	Forest	Agriculture	Built-up	Bare soil	Water
10	NDVI	0.4-0.65	0.3-0.4	0.25-0.3	0.14-0.25	-0.1-0.14

* Notes: Class numbers 1, 2, 3, 4, and 5 indicate the degree of very low, low, moderate, high, and very high influence on flash floods.
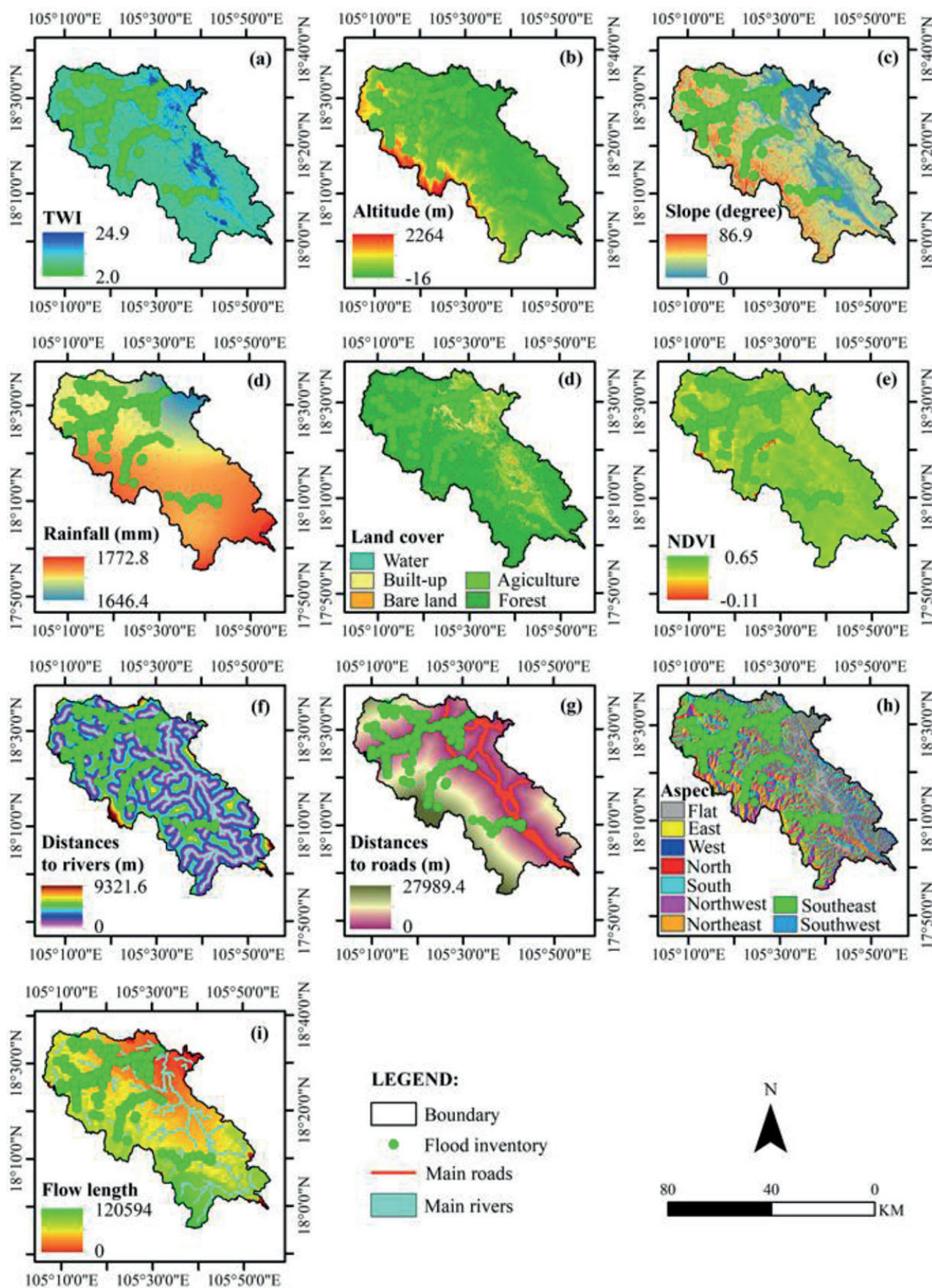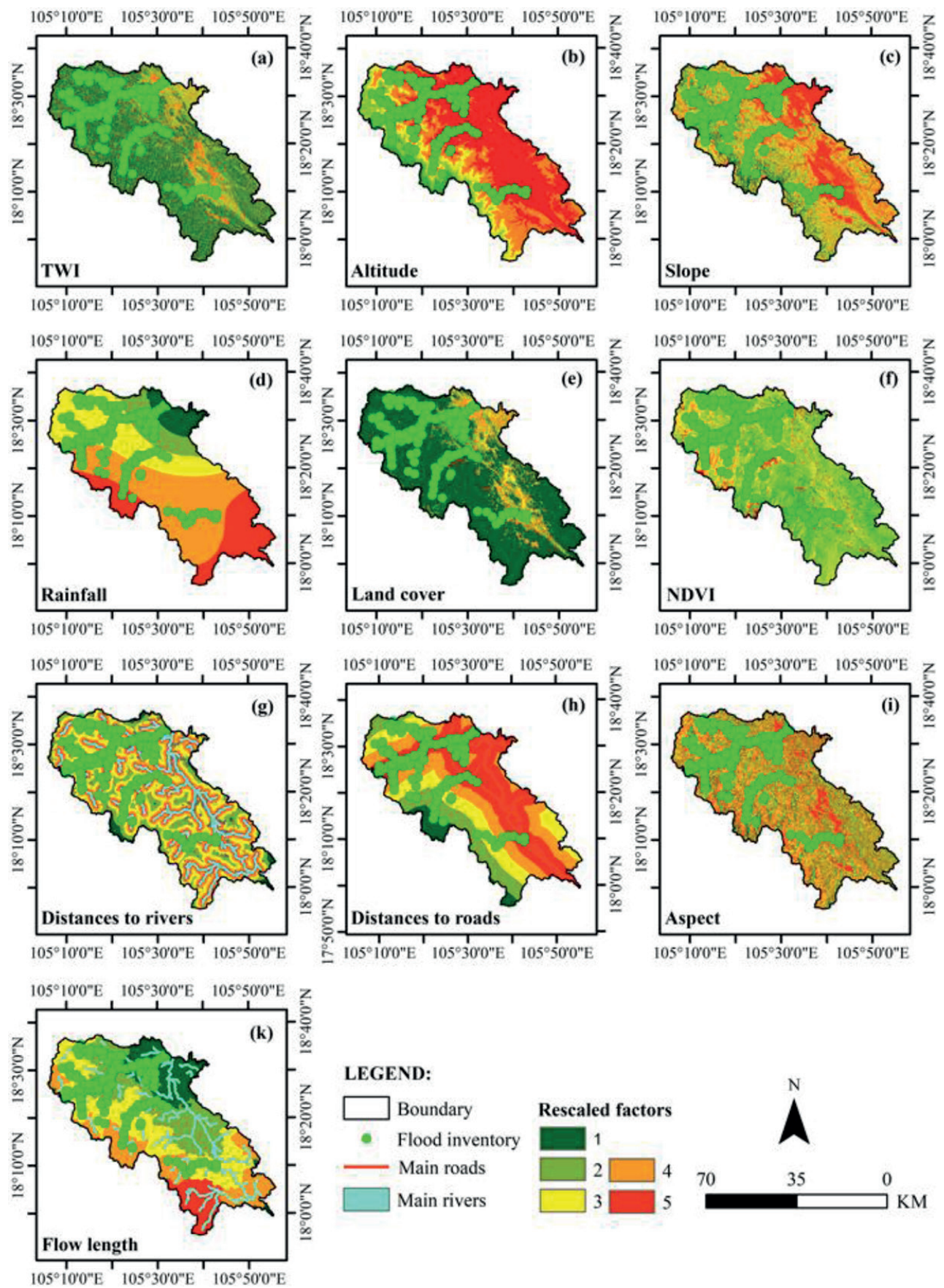
Fig. 3. Maps of 10 influencing factors

Fig. 4. Maps of ten rescaled influencing factors

experts, the pairwise comparison matrix was formed (Table 2). The AHP technique was then employed to identify the corresponding weight of each influencing factor. Data from Table 2 illustrates the weight values of influencing factors that were obtained from AHP. The Consistency Ratio (CR) of 5.5% was within the limits of 10% (CR < 0.01). This proves the expert's consistency and the validity of the computed weights. Therefore, there is no need to repeat the evaluations. A higher weight value of the factors represents the corresponding factors having more influence on flash floods than others within the Ngan Sau and Ngan Pho study area. Data from Table 2 demonstrates that, with the highest weights of 0.14, two factors, namely distance from rivers and TWI, have the greatest influence on flooding in the study area. These two factors are characterized by the position, the direction, and the accumulation of water flow. It is followed by the rainfall and altitude factors with corresponding weights of 0.13 and 0.12, respectively. This implies that after distance from rivers and TWI factors, rainfall and altitude make more of a contribution to flooding in the area as compared to the remaining factors. This rainfall factor-related result was consistent with those reported by Nguyen (2017) that rainfall duration and intensity in the period of 1990-2012 caused floods in 2002 2007, and 2010 in this area (Hoang et al. 2020; Nguyen 2017). Slope, aspect, flow length, and LULC, with the corresponding weights of 0.1, 0.09, 0.09, and 0.07, respectively, are factors having less influence as compared with the factors discussed above. The lowest weight values of 0.06 were found for both the distance from roads and NDVI factors. This indicates that these two factors have the least influence on flooding in the study area.

Analysis of flash flood hazards

The use of 151 flood inventory sites for the validation of the flash flood hazards in the Ngan Sau and Ngan Pho river basins has revealed that a total of 84.8 percent of flood inventory sites were in good conformity with moderate to very high levels of flash flood hazard areas. This indicates a high degree of strong spatial correlation. In particular, a higher degree of correlation between flood inventory areas and moderate-to-high level flash flood hazard areas obtained from the proposed method was found in the Ngan Sau River basin, in the northern and northwestern

study areas (Fig. 5). This result suggests that the integration of Landsat-8 imagery, GIS and AHP allows for accurate and reliable flash flood hazard mapping in this study area.

The areas of flash flood hazards in the Ngan Sau and Ngan Pho river basins were statistically summarized in Table 3 and their corresponding spatial distribution was shown in Fig. 5, respectively. Data from Table 3 illustrates the areas of very high and high flash flood hazard levels were 275 and 621.1 km², accounting for 19.5 and 8.6 percent of the total areas of the river basin, respectively. Moderate, low, and very low flash flood hazard levels were extracted with areas of 923.2, 889.1, and 477.8 km², accounting for most of the total area with 29, 27.9, and 15 percent, respectively. Data from Fig. 5 demonstrates the very high and high flash flood hazard levels. They were mainly located in the areas along and close to the main Ngan Sau and Ngan Pho rivers and streams, whereas the moderate, low, and very low flood hazard levels were mostly detected in the areas of high and very high altitudes and far from rivers and roads. It is clear that there was a strong correlation between areas of high, very high flash flood hazard levels and close distances to rivers and high TWI areas. In particular, the results on high and very high levels of flash flood hazard areas are in good agreement with the locations of floods recorded and reported in recent studies in the districts of Huong Son in 2016 and 2017 (Hoang et al. 2020; Nguyen and Ha 2017; Nguyen 2017; PSN 2016) and of Duc Tho in 2017 (Group 2016; Thien 2017) in the northwest and northeast of the river basin. High and very high levels of flash flood hazard areas were also identified in Vu Quang district in the west of the basin where flash floods often hit in flood seasons such as in 2011 (Minh Thu 2011) and 2017 (Tien 2017). In addition, moderate-to-very high levels of flash flood hazards were found in the area of Huong Khe district, southwest of the river basin. These areas of flash flood hazards were in good conformity with flash flood sites reported in recent studies such as in 2013 (VT 2019). A negative correlation between low and very low flash flood hazard areas and flood inventory sites. This is consistent with the fact that no floods in history were reported and occurred in very low and low-flash flood hazard areas.

Table 2. Ranking of flash flood influencing factors to obtain the pairwise comparison matrix and their corresponding weights

Comparison Matrix											Weights
Influencing factors	1	2	3	4	5	6	7	8	9	10	
TWI	1	1	1	1	3	5	1	3	1	1	0.14
Altitude	1	1	1	1	2	3	1	3	1	1	0.12
Slope	1	1	1	1	3	1	1/2	1	1	1	0.10
Rainfall	1	1	1	1	3	2	2	3	1	1	0.13
LULC	1/3	1/2	1/3	1/3	1	1	1/3	3	1	1	0.07
NDVI	1/5	1/3	1	1/2	1	1	1/5	1	1	1	0.06
Distance from rivers	1	1	2	1/2	3	5	1	3	1	1	0.14
Distance from roads	1/3	1/3	1	1/3	1/3	1	1/3	1	1	1	0.06
Aspect	1	1	1	1	1	1	1	1	1	1	0.09
Flow length	1	1	1	1	1	1	1	1	1	1	0.09
Consistency Ratio = 5.5% (< 10%)											

Table 3. Areas of flash flood hazard levels

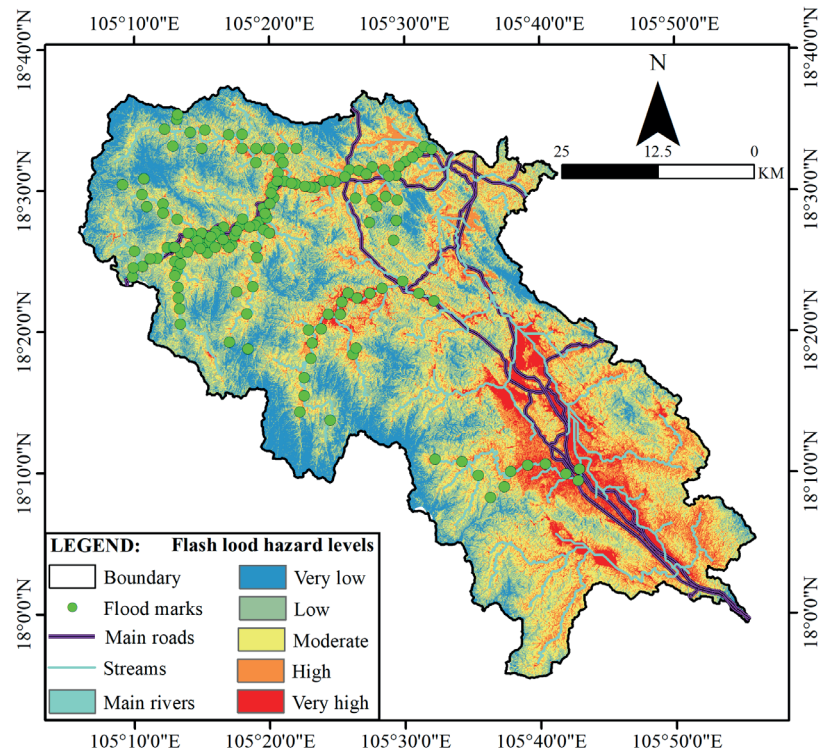| Levels of flash flood hazards	Areas [km²]	Percentage [%]	Accumulated percentage [%]
Very low	477.8	15.0	15.0
Low	889.1	27.9	42.9
Moderate	923.2	29.0	71.9
High	621.1	19.5	91.4
Very high	275.0	8.6	100.0

Fig. 5. Map of flash flood hazards

CONCLUSIONS

This study set out to investigate the integration of Landsat-8 imagery, AHP, and GIS in mapping flash flood hazards in the Ngan Sau and Ngan Pho river basins, in north-central Vietnam. A total of ten exploratory factors influencing the flash flood hazards occurrence, namely TWI, altitude, slope, aspect, rainfall, land cover, NDVI, distances to rivers and roads, and flow length, were used to calculate the weights with the help of the AHP technique. Land cover and NDVI were extracted from Landsat-8 OLI imagery. Methods for spatial analysis in GIS were then applied to map the flood hazard. Finally, the validation was carried out using 151 flood inventory sites. The study's results indicated that flash flood hazards are mainly associated with distance from rivers, TWI, and rainfall factors. In addition, a high degree of spatial correlation between 128 flood inventory sites and moderate to very high levels of flash flood hazard areas were also revealed. Last but not least, high and very high flood hazard levels were mainly detected along and close to the main rivers and streams, with areas of 275 and 621.1 km², respectively. All these results confirm the effectiveness of the Landsat-8 imagery, AHP, and GIS combination in providing practical flash flood hazard maps. These findings from this study not only enable better watershed management but also effectively reduce the likelihood of future flooding. One source of weakness in this study which could have affected the accuracy of the proposed method was the lack of the factor of rainfall threshold for flash floods. Therefore, more research is required to fully understand how this aspect affects the identification of flash flood hazards.

AUTHOR CONTRIBUTIONS

Tien-thanh Nguyen designed the research, processed and analyzed the data, analysed the findings, and produced the report. Thi-thu-huong Pham and Thi-thu-trang Tran collected the data. The authors revised the manuscript under the supervision of Anh-huy Hoang. All authors discussed the findings and offered feedback on the manuscript at all stages. ■

REFERENCES

Abou El-Magd I., Hermas E. and El Bastawesy M. (2010). GIS-modelling of the spatial variability of flash flood hazard in Abu Dabbab catchment, Red Sea Region, Egypt. The Egyptian Journal of Remote Sensing and Space Science, 13(1), 81–88, DOI: 10.1016/j.ejrs.2010.07.010.

Alvarez-Mendoza C.I., Teodoro A. and Ramirez-Cando L. (2019). Improving NDVI by removing cirrus clouds with optical remote sensing data from Landsat-8–a case study in Quito, Ecuador. Remote Sensing Applications: Society and Environment, 13, 257–274, DOI: 10.1016/j.rsase.2018.11.008.

Arabameri A., Rezaei K., Cerdà A., Conoscenti C. and Kalantari Z. (2019). A comparison of statistical methods and multi-criteria decision making to map flood hazard susceptibility in Northern Iran. Science of the Total Environment, 660, 443–458, DOI: 10.1016/j.scitotenv.2019.01.021.

Aydin M.C. and Sevgi Birincioğlu E. (2022). Flood risk analysis using gis-based analytical hierarchy process: a case study of Bitlis Province. Applied Water Science, 12(6), 122, DOI: 10.1007/s13201-022-01655-x.

Bich T.H., Quang L.N., Thanh Ha L.T., Duc Hanh T.T. and Guha-Sapir D. (2011). Impacts of flood on health: epidemiologic evidence from Hanoi, Vietnam. Global Health Action, 4(1), 6356, DOI: 10.3402/gha.v4i0.6356.

Bui D.T., Hoang N.-D., Martínez-Álvarez F., Ngo P.-T.T., Hoa P.V., Pham T.D., Samui P. and Costache R. (2020). A novel deep learning neural network approach for predicting flash flood susceptibility: A case study at a high frequency tropical storm area. Science of The Total Environment, 701, 134-413, DOI: 10.1016/j.scitotenv.2019.134413.

Chang D.-L., Yang S.-H., Hsieh S.-L., Wang H.-J. and Yeh K.-C. (2020). Artificial intelligence methodologies applied to prompt pluvial flood estimation and prediction. Water, 12(12), 35-52, DOI:10.3390/w12123552.

Chapi K., Singh V.P., Shirzadi A., Shahabi H., Bui D.T., Pham B.T. and Khosravi K. (2017). A novel hybrid artificial intelligence approach for flood susceptibility assessment. Environmental Modelling and Software, 95, 229–245, DOI: 10.1016/J.ENVSOFT.2017.06.012.

Chatzichristaki C., Stefanidis S., Stefanidis P. and Stathis D. (2015). Analysis of the flash flood in Rhodes Island (South Greece) on 22 November 2013. Silva, 16(1), 76–86.

Chen W., Hong H., Li S., Shahabi H., Wang Y., Wang X. and Ahmad B. Bin. (2019). Flood susceptibility modelling using novel hybrid approach of reduced-error pruning trees with bagging and random subspace ensembles. Journal of Hydrology, 575, 864–873, DOI: 10.1016/j.jhydrol.2019.05.089.

Chowdhuri I., Pal S.C. and Chakrabortty R. (2020). Flood susceptibility mapping by ensemble evidential belief function and binomial logistic regression model on river basin of eastern India. Advances in Space Research, 65(5), 1466–1489, DOI: 10.1016/j.asr.2019.12.003.

Costache R., Tin T.T., Arabameri A., Crăciun A., Ajin R.S., Costache I., Islam A.R.M.T., Abba S.I., Sahana M. and Avand M. (2022). Flash-flood hazard using deep learning based on H2O R package and fuzzy-multicriteria decision-making analysis. Journal of Hydrology, 609, 127-747, DOI: 10.1016/j.jhydrol.2022.127747.

Daneshparvar B., Rasi Nezami S., Feizi A. and Aghlmand R. (2022). Comparison of results of flood hazard zoning using AHP and ANP methods in GIS environment: A case study in Ardabil province, Iran. Journal of Applied Research in Water and Wastewater, 9(1), 1–7, DOI: 10.22126/ARWW.2022.6667.1218.

Field C.B., Barros V., Stocker T.F. and Dahe Q. (2012). Managing the risks of extreme events and disasters to advance climate change adaptation: special report of the intergovernmental panel on climate change. Cambridge University Press, DOI: 10.13140/2.1.3117.9529.

Gaume E., Bain V., Bernardara P., Newinger O., Barbuc M., Bateman A., Blaškovičová L., Blöschl G., Borga M. and Dumitrescu A. (2009). A compilation of data on European flash floods. Journal of Hydrology, 367(1–2), 70–78, DOI: 10.1016/J.JHYDROL.2008.12.028.

Getahun Y.S. and Gebre S.L. (2015). Flood hazard assessment and mapping of flood inundation area of the Awash River Basin in Ethiopia using GIS and HEC-GeoRAS/HEC-RAS model. Journal of Civil and Environmental Engineering, 5(4), 1, DOI: 10.4172/2165-784X.1000179.

Gigović L., Pamučar D., Bajić Z. and Drobnjak S. (2017). Application of GIS-interval rough AHP methodology for flood hazard mapping in urban areas. Water, 9(6), 360, DOI: 10.3390/w9060360.

Group B. (2016). Golden heart fund relieved flood victims in Ha Tinh province. Bitexco Group [online]. Available at: http://bitexco.com.vn/newdetail/golden-heart-fund-relieved-flood-victims-in-ha-tinh-province-115.html [Accessed 6 Nov. 2021].

Hoang L.T.T. and Tran T.M. (2018). Climate Change Vulnerability Assessment Fortourism Sector in Ha Tinh Province. VNU Journal of Science: Earth and Environmental Sciences, 34(1), DOI: 10.25073/2588-1094/vnuees.4230.

Hoang V., Tran H.T. and Nguyen T.T. (2020). A GIS-based spatial multi-criteria approach for flash flood risk assessment in the ngan sau-ngan PHO mountainous river basin, north central of Vietnam. Environment and Natural Resources Journal, 18(2), DOI: 10.32526/ennrj.18.2.2020.11.

Hosseini F.S., Choubin B., Mosavi A., Nabipour N., Shamshirband S., Darabi H. and Haghighi A.T. (2020). Flash-flood hazard assessment using ensembles and Bayesian-based machine learning models: Application of the simulated annealing feature selection method. Science of the Total Environment, 711, 135-161, DOI: 10.1016/j.scitotenv.2019.135161.

Jonkman S.N. (2005). Global perspectives on loss of human life caused by floods. Natural Hazards, 34(2), 151–175, DOI: 10.1007/s11069-004-8891-3.

Kha D.D., Nhu N.Y. and Anh T.N. (2018). An approach for flow forecasting in ungauged catchments–A case study for Ho Ho reservoir catchment, Ngan Sau River, Central Vietnam. Journal of Ecological Engineering 19(3), 74–79, DOI: 10.12911/22998993/85759.

Koem C. and Tantanee S. (2021). Flash flood hazard mapping based on AHP with GIS and satellite information in Kampong Speu Province, Cambodia. International Journal of Disaster Resilience in the Built Environment, 12(5), 457–470, DOI: 10.1108/IJDRBE-09-2020-0099.

Koks E.E., Jongman B., Husby T.G. and Botzen W.J.W. (2015). Combining hazard, exposure and social vulnerability to provide lessons for flood risk management. Environmental Science and Policy, 47(2), 42–52, DOI: 10.1016/j.envsci.2014.10.013.

Kvočka D., Falconer R.A. and Bray M. (2016). Flood hazard assessment for extreme flood events. Natural Hazards, 84(3), 1569–1599, DOI: 10.1007/s11069-016-2501-z.

Long B.D. and Dung P.T. (2009). Flash floods, hydrometeorological forecasting and warning systems in Viet Nam. Proceedings of the 7th Annual Mekong Flood Forum: Integrated Flood Risk Management in the Mekong River Basin, 229–240.

Lootsma F.A. (1999). Multi-criteria decision analysis via ratio and difference judgement. Springer, DOI: 10.1007/b102374.

Malik S., Pal S.C., Arabameri A., Chowdhuri I., Saha A., Chakrabortty R., Roy P. and Das B. (2021). GIS-based statistical model for the prediction of flood hazard susceptibility. Environment, Development and Sustainability, 23, 16713–16743, DOI: 10.1007/s10668-021-01377-1.

Marzouki A. and Dridri A. (2022). Normalized Difference Enhanced Sand Index for desert sand dunes detection using Sentinel-2 and Landsat 8 OLI data, application to the north of Figuig, Morocco. Journal of Arid Environments 198, 104-693, DOI: 10.1016/j.jaridenv.2021.104693.

Merz B., Blöschl G., Vorogushyn S., Dottori F., Aerts J.C.J.H., Bates P., Bertola M., Kemter M., Kreibich H. and Lall U. (2021). Causes, impacts and patterns of disastrous river floods. Nature Reviews Earth and Environment, 2(9), 592–609.

Minh Thu C.T. (2011). Spring buds after floods [online]. Nhan Dan Online. Available at: https://en.nhandan.vn/spring-buds-after-floods-post15790.html [Accessed 6 Nov. 2021].

Mudashiru R.B., Sabtu N., Abdullah R., Saleh A. and Abustan I. (2022). A comparison of three multi-criteria decision-making models in mapping flood hazard areas of Northeast Penang, Malaysia. Natural Hazards, 112(3) 1903–1939, DOI: 10.1007/s11069-022-05250-w.

Mudashiru R.B., Sabtu N., Abustan I. and Balogun W. (2021). Flood hazard mapping methods: A review. Journal of Hydrology, 603, 126846.

Mukherjee F. and Singh D. (2020). Detecting flood prone areas in Harris County: a GIS based analysis. GeoJournal, 85(3), 647–663, DOI: 10.1007/s10708-019-09984-2.

Neji N., Ayed R. Ben and Abida H. (2021). Water erosion hazard mapping using analytic hierarchy process (AHP) and fuzzy logic modeling: a case study of the Chaffar Watershed (Southeastern Tunisia). Arabian Journal of Geosciences, 14, 1–15, DOI: 10.1007/s12517-021-07602-5.

Nguyen D. and Ha H.Q. (2017). Flash floods potential area mapping at Huong Khe District, Ha Tinh prov. VNUHCM Journal of Natural Sciences, 1(T4), 249–254, DOI: 10.32508/stdjns.v1iT4.487.

Nguyen H. (2017). Thousands of households violated by a flood in Ha Tinh province [online]. Dai Doan Ket Newspaper. Available at: http://daidoanket.vn/xa-hoi/ha-tinh-hang-nghin-ho-dan-bi-ngap-lut-tintuc382249 [Accessed 6 Nov. 2021].

Noy I. and Vu T.B. (2010). The economics of natural disasters in a developing country: The case of Vietnam. Journal of Asian Economics, 21(4), 345–354, DOI: 10.1016/j.asieco.2010.03.002.

Park S. and Kim J. (2019). Landslide susceptibility mapping based on random forest and boosted regression tree models, and a comparison of their performance. Applied Sciences, 9(5), 942, DOI: 10.3390/app9050942.

Pathan A.I., Girish Agnihotri P., Said S. and Patel D. (2022). AHP and TOPSIS based flood risk assessment-a case study of the Navsari City, Gujarat, India. Environmental Monitoring and Assessment, 194(7), 509.

Prokešová R., Horáčková Š. and Snopková Z. (2022). Surface runoff response to long-term land use changes: Spatial rearrangement of runoff-generating areas reveals a shift in flash flood drivers. Science of the Total Environment, 815, 151-591, DOI: 10.1016/j.scitotenv.2021.151591.

PSN. (2016). People's Police College 5 supports people in flood-hit localities [online]. Public Security News. Available at: http://en.cand.com.vn/Public-security-forces/People-s-Police-College-5-supports-people-in-flood-hit-localities-414865/ [Accessed 6 Nov. 2021].

Qiang Y. (2019). Flood exposure of critical infrastructures in the United States. International Journal of Disaster Risk Reduction, 39, 101-240, DOI: 10.1016/j.ijdrr.2019.101240.

Rahman M., Chen N., Islam M.M., Mahmud G.I., Pourghasemi H.R., Alam M., Rahim M.A., Baig M.A., Bhattacharjee A. and Dewan A. (2021). Development of flood hazard map and emergency relief operation system using hydrodynamic modeling and machine learning algorithm. Journal of Cleaner Production, 311, 127594, DOI: 10.1016/j.jclepro.2021.127594.

Rahman M., Ningsheng C., Mahmud G.I., Islam M.M., Pourghasemi H.R., Ahmad H., Habumugisha J.M., Washakh R.M.A., Alam M. and Liu E. (2021). Flooding and its relationship with land cover change, population growth, and road density. Geoscience Frontiers, 12(6), 101224, DOI: 10.1016/j.gsf.2021.101224.

Rehman A., Song J., Haq F., Mahmood S., Ahamad M.I., Basharat M., Sajid M. and Mehmood M.S. (2022). Multi-hazard susceptibility assessment using the analytical hierarchy process and frequency ratio techniques in the Northwest Himalayas, Pakistan. Remote Sensing, 14(3), 554, DOI: 10.3390/rs14030554.

Saaty, T.L. (1988). What is the Analytic Hierarchy Process? Mathematical Models for Decision Support. NATO ASI Series, Springer, Berlin, Heidelberg, 48, DOI: 10.1007/978-3-642-83555-1_5.

Şahin M. (2021). A comprehensive analysis of weighting and multicriteria methods in the context of sustainable energy. International Journal of Environmental Science and Technology, 18(6), 1591–1616, DOI: 10.1007/s13762-020-02922-7.

Satarzadeh E., Sarraf A., Hajikandi H. and Sadeghian M.S. (2022). Flood hazard mapping in western Iran: assessment of deep learning vis-à-vis machine learning models. Natural Hazards, 1–19, DOI: 10.1007/s11069-021-05098-6.

Stefanidis S., Alexandridis V. and Theodoridou T. (2022). Flood exposure of residential areas and infrastructure in Greece. Hydrology, 9(8), 145, DOI: 10.3390/hydrology9080145.

Tehrany M.S., Pradhan B. and Jebur M.N. (2015). Flood susceptibility analysis and its verification using a novel ensemble support vector machine and frequency ratio method. Stochastic Environmental Research and Risk Assessment, 29, 1149–1165, DOI: 10.1007/s00477-015-1021-9.

Teng J., Jakeman A.J., Vaze J., Croke B.F.W., Dutta D. and Kim S. (2017). Flood inundation modelling: A review of methods, recent advances and uncertainty analysis. Environmental Modelling and Software, 90 201–216, DOI: 10.1016/J.ENVSOFT.2017.01.006.

Thien D. (2017). Flash flood in Duc Tho distric, Ha Tinh province [online]. Ha Tinh Newspaper. Available at: https://baohatinh.vn/xa-hoi/hung-lu-thuong-nguon-ve-vung-ngoai-de-duc-tho-ngap-bang/141928.htm [Accessed 6 Nov. 2021].

Tien D. (2017). Police forces help people overcome floods. Ministry of Public Security of Socialist Republic of Vietnam [online]. Available at: https://en.bocongan.gov.vn/social-ativities/police-forces-help-people-overcome-floods-t4209.html [Accessed 6 Nov. 2021].

VT H. (2019). Emergency response to flood in Huong Son, Ha Tinh. [online]. Available at: https://www.oxfamblogs.org/vietnam/2014/01/29/emergency-response-to-flood-in-huong-son-ha-tinh/ [Accessed 6 Nov. 2021].